

**Supporting Information for**

**“A  $^{115}\text{In}$  Solid-State NMR Study of Low-Oxidation State Indium Complexes”**

by Hiyam Hamaed,<sup>1</sup> Karen E. Johnston,<sup>1</sup> Benjamin F. T. Cooper,<sup>1</sup> Victor V. Terskikh,<sup>2</sup> Eric Ye,<sup>3</sup> Charles L. B. Macdonald,<sup>1</sup> Donna C. Arnold,<sup>4</sup> and Robert W. Schurko<sup>1,\*</sup>

<sup>1</sup>Department of Chemistry and Biochemistry, University of Windsor, Windsor, Ontario, Canada, N9B 3P4; <sup>2</sup>Steacie Institute for Molecular Sciences, National Research Council Canada, Ottawa, Ontario, Canada, K1A 0R6; <sup>3</sup>Department of Chemistry, University of Ottawa, Ottawa, Ontario, Canada, K1N 6N5, <sup>4</sup>School of Physical Sciences, University of Kent, Canterbury, Kent, United Kingdom, CT2 7NH

\*Author to whom correspondence should be addressed

Phone: (519) 253-3000 x3548. Fax: (519) 973-7098. Email: rschurko@uwindsor.ca

**Table of Contents:**

Table S1. $^{115}\text{In}$ NMR experimental parameters at 9.4 T	S2
Table S2. $^{115}\text{In}$ NMR experimental parameters at 21.1 T	S2
Table S3. $^{115}\text{In}$ MAS NMR experimental parameters at 21.1 T	S2
Figure S1. The contribution of $^{115}\text{In}$ CSA on the NMR pattern of $[\text{In}][\text{GaCl}_4]$	S3
Figure S2. The contribution of $^{115}\text{In}$ CSA on the NMR pattern of $\text{InI}$	S4
Figure S3. The contribution of $^{115}\text{In}$ CSA on the NMR pattern of $\text{InBr}$	S5
Figure S4. Simulation of $^{115}\text{In}$ NMR pattern of $[\text{In}][\text{OTf}]$ at 9.4 T with parameters of two indium sites	S6
Figure S5. The contribution of $^{115}\text{In}$ CSA on the NMR pattern of $[\text{In}][\text{OTf}]$	S7
Figure S6. The contribution of $^{115}\text{In}$ CSA on the NMR pattern of $[\text{In}(15\text{-crown-5})_2][\text{OTf}]$	S8
Figure S7. The contribution of $^{115}\text{In}$ CSA on the NMR pattern of $[\text{In}(15\text{-crown-6})][\text{OTf}]$	S9
Figure S8. pXRD patterns for $[\text{In}(18\text{-crown-6})][\text{GaCl}_4]$ and $[\text{In}(18\text{-crown-6})][\text{AlCl}_4]$	S10
Figure S9. The contribution of $^{115}\text{In}$ CSA on the NMR pattern of $[\text{In}(18\text{-crown-6})][\text{GaCl}_4]$	S11
Figure S10. The contribution of $^{115}\text{In}$ CSA on the NMR pattern of $[\text{In}(18\text{-crown-6})][\text{AlCl}_4]$	S12
Figure S11. Static $^{71}\text{Ga}$ SSNMR spectrum of $[\text{In}(18\text{-crown-6})][\text{GaCl}_4]$ and $^{27}\text{Al}$ SSNMR spectra of $\text{AlCl}_4$ and $[\text{In}(18\text{-crown-6})][\text{AlCl}_4]$ at 9.4 T	S13
Figure S12. $^{13}\text{C}$ MAS NMR spectra of $[\text{In}(15\text{-crown-5})_2][\text{OTf}]$ at 21 °C and at 45 °C	S14
Figure S13. $^1\text{H}$ MAS NMR spectra of $[\text{In}(15\text{-crown-5})_2][\text{OTf}]$ at 21 °C and at 45 °C	S15
Figure S14. $^{115}\text{In}$ NS tensor orientations	S16

**Table S1.**  $^{115}\text{In}$  Static NMR Experimental Parameters at 9.4 T

	rf power (kHz)	Recycle Delay (s)	Spectral Width (kHz)	Number of Subspectra	Offset Frequency (kHz)	Number of Scans per Subspectrum
[In][GaCl <sub>4</sub> ]	67	0.1	1000	1	-	8544
[In([15]crown-5) <sub>2</sub> ][OTf]	77	0.1	1000	1	-	579152
[In([18]crown-6)][GaCl <sub>4</sub> ]	111	0.1	1000	3	150	18848
[In([18]crown-6)][AlCl <sub>4</sub> ]	111	0.1	1000	3	150	66288
InI	67	0.1	2000	6	100	17824
InBr	67	0.1	2000	8	125	8544
WURST-Echo						
[In][OTf]	17	0.1	2000	5	250	15736

**Table S2.**  $^{115}\text{In}$  Static NMR Experimental Parameters at 21.1 T

	rf power (kHz)	Recycle Delay (s)	Spectral Width (kHz)	Number of Subspectra	Offset Frequency (kHz)	Number of Scans per Subspectrum
[In][GaCl <sub>4</sub> ]	50	1	200	1	-	1024
[In([15]crown-5) <sub>2</sub> ][OTf]	50	1	200	1	-	2976
[In([18]crown-6)][GaCl <sub>4</sub> ]	50	1	500	1	60	2048
[In([18]crown-6)][AlCl <sub>4</sub> ]	50	1	500	1	60	16384
[In([18]crown-6)][OTf]	100	1	2000	1	-	6144
[In][OTf]	50	1	1000	3	120	2048
InI	50	1	500	1	-	1782
InBr	50	1	1000	1	-	5557

**Table S3.**  $^{115}\text{In}$  MAS NMR Experimental Parameters at 21.1 T

	v <sub>rot</sub> (kHz)	rf power (kHz)	Recycle Delay (s)	Spectral Width (kHz)	Number of Scans
[In][GaCl <sub>4</sub> ]	18	50	1	200	2200
[In([15]crown-5) <sub>2</sub> ][OTf]	12.5	50	0.5	200	4096
[In([18]crown-6)][GaCl <sub>4</sub> ]	50	100	0.5	1000	20480
[In([18]crown-6)][AlCl <sub>4</sub> ]	50	100	0.5	1000	136000
[In][OTf]	62.5	100	0.5	1000	16000
InI	62.5	100	0.5	1000	10240
InBr	62.5	100	0.5	1000	16400

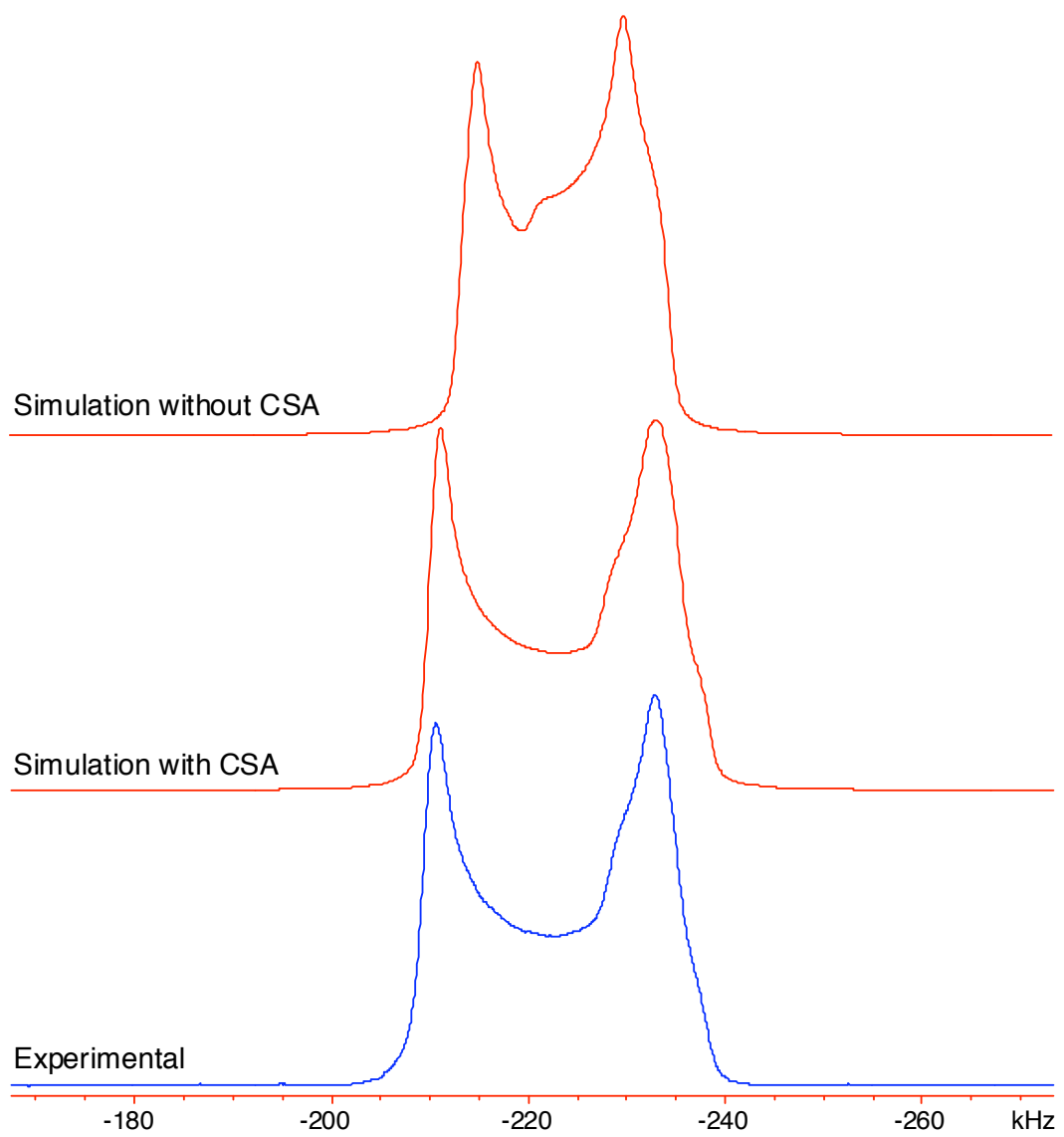


**Figure S1.** The contribution of  $^{115}\text{In}$  CSA on the NMR pattern of  $[\text{In}][\text{GaCl}_4]$  acquired at 21.1 T.

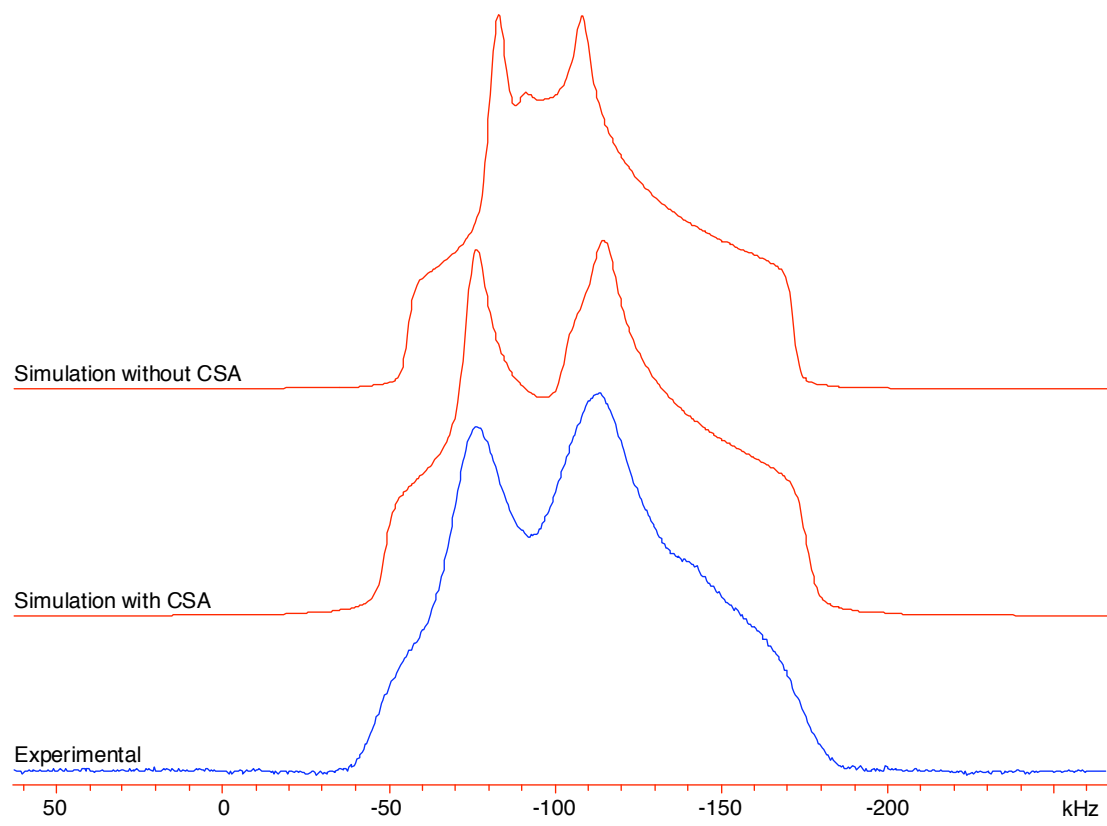


**Figure S2.** The contribution of  $^{115}\text{In}$  CSA on the NMR pattern of InI acquired at 21.1 T.

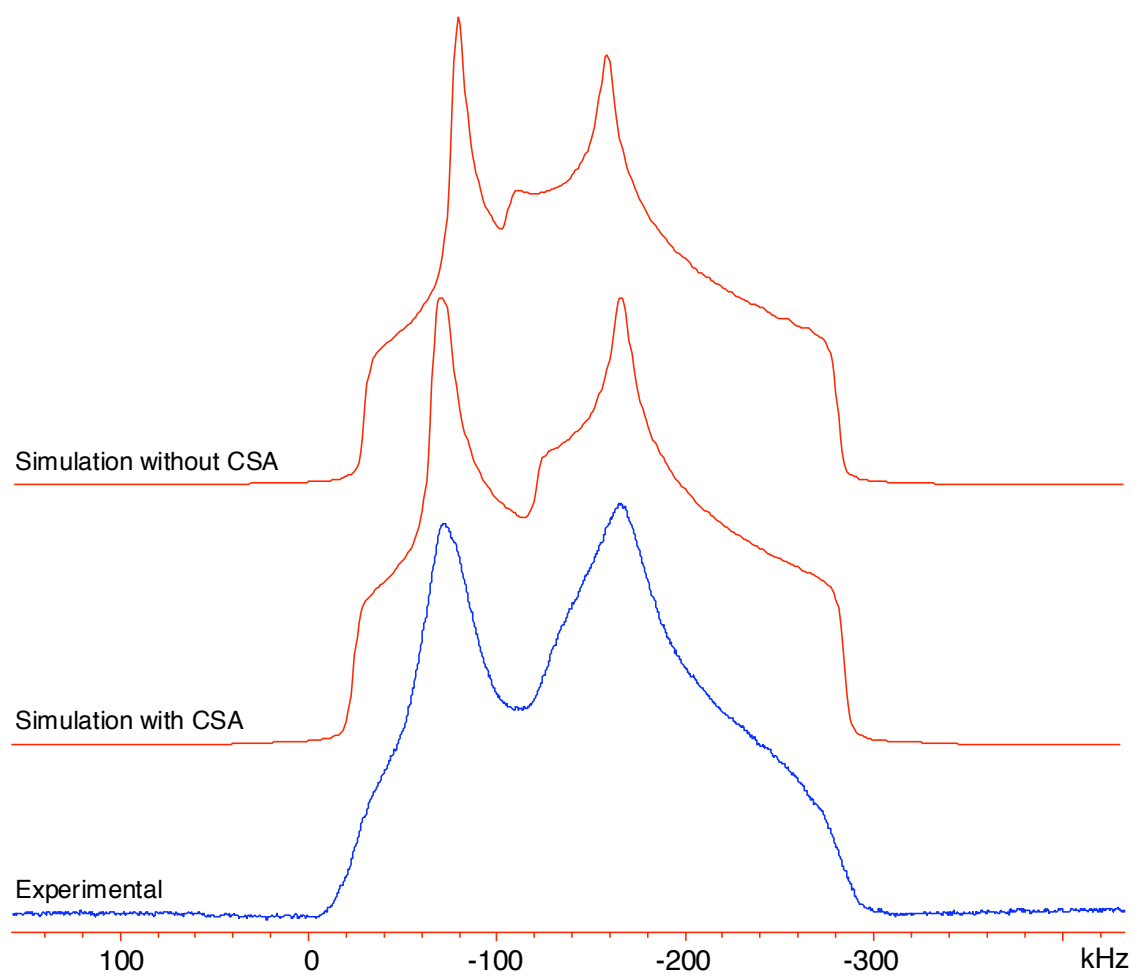


**Figure S3.** The contribution of  $^{115}\text{In}$  CSA on the NMR pattern of InBr acquired at 21.1 T.

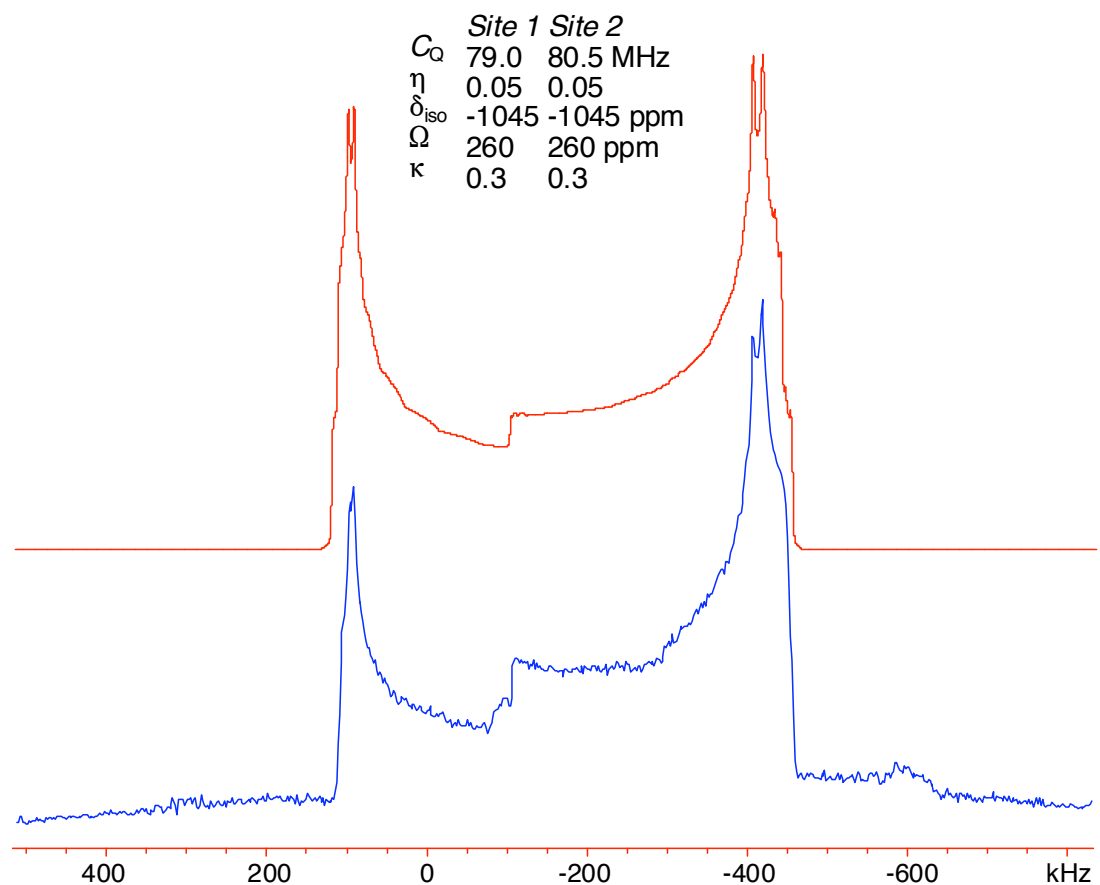


**Figure S4.** Simulation (top) of  $^{115}\text{In}$  NMR pattern (bottom) of  $[\text{In}][\text{OTf}]$  at 9.4 T with parameters of two indium sites.

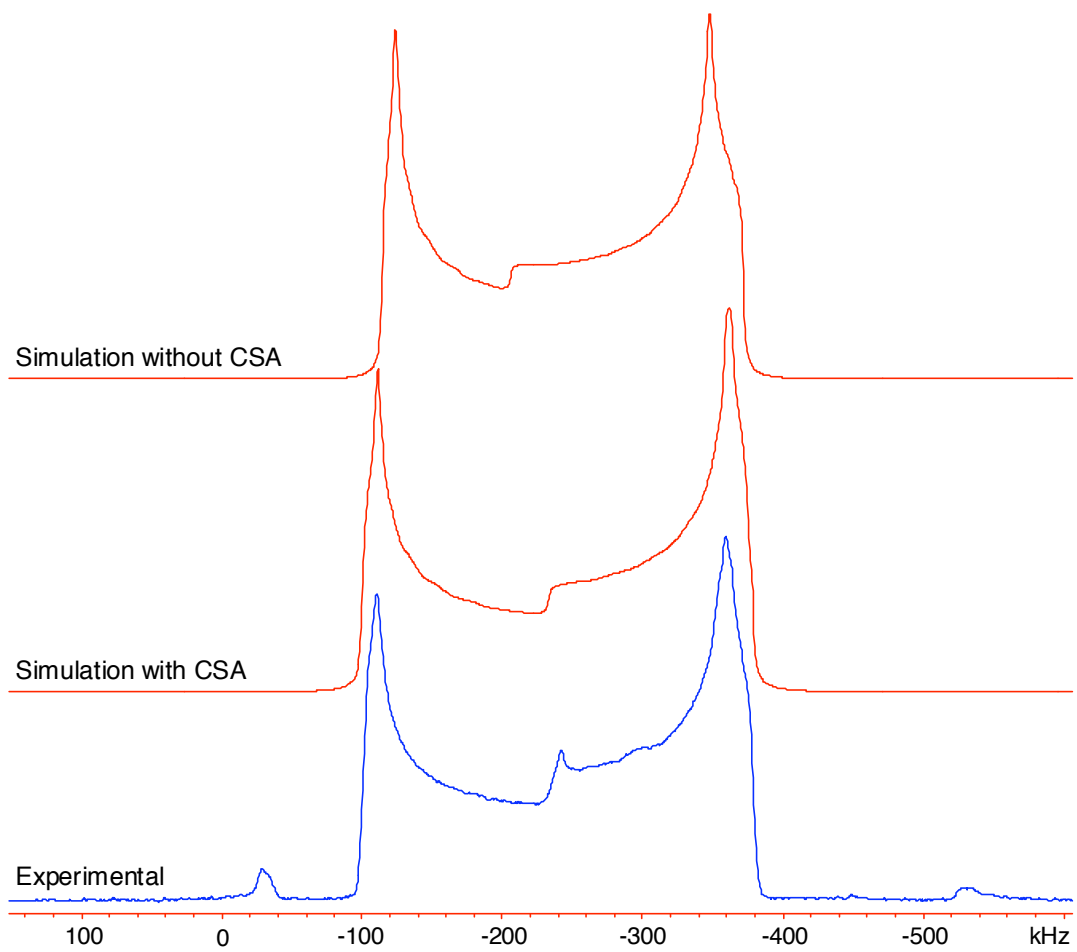


**Figure S5.** The contribution of  $^{115}\text{In}$  CSA on the NMR pattern of  $[\text{In}][\text{OTf}]$  acquired at 21.1 T.

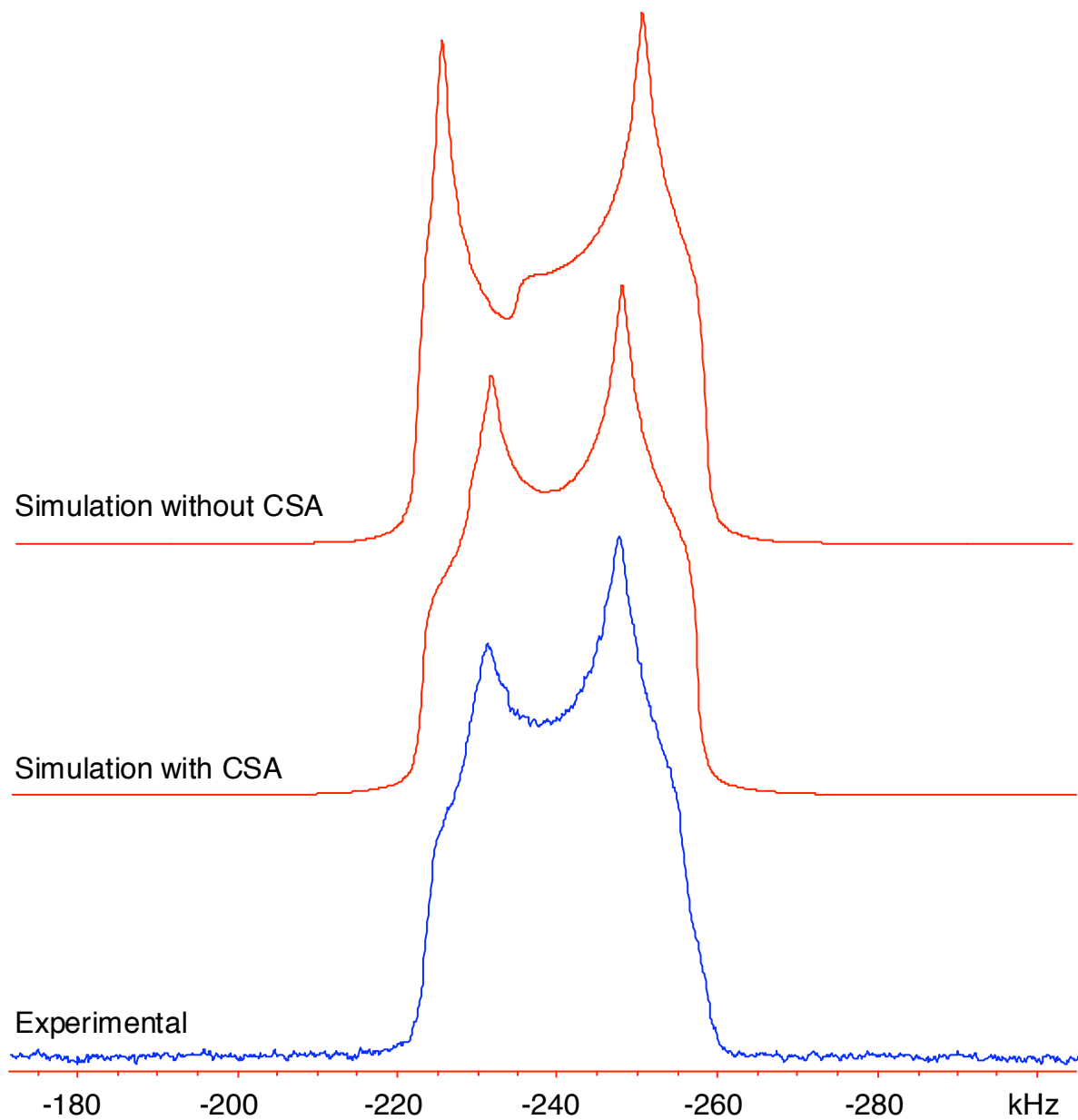


**Figure S6.** The contribution of  $^{115}\text{In}$  CSA on the NMR pattern of  $[\text{In}([\text{15}] \text{crown-5})_2]\text{[OTf]}$  acquired at 21.1 T.

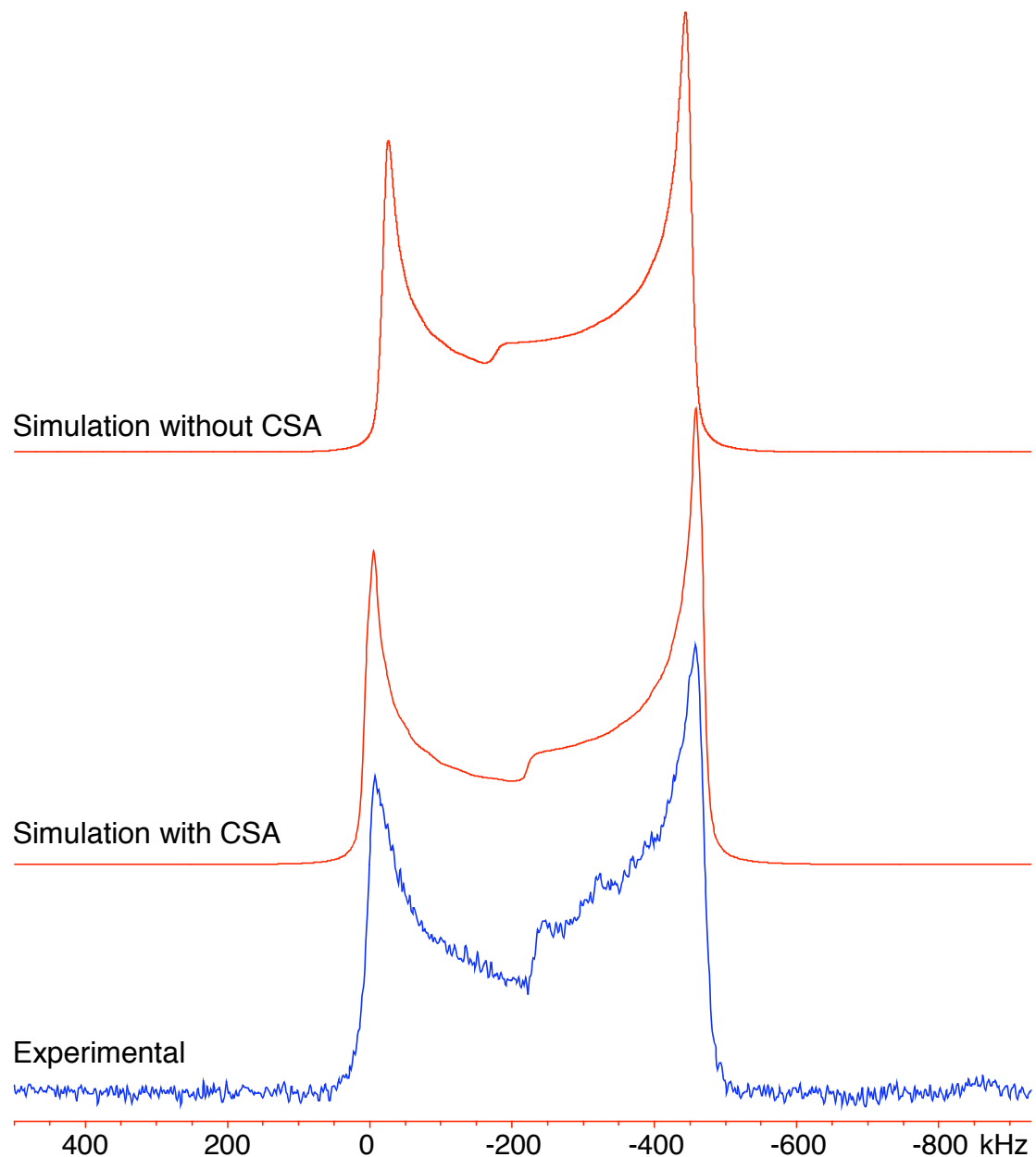


**Figure S7.** The contribution of  $^{115}\text{In}$  CSA on the NMR pattern of  $[\text{In}([\text{18}] \text{crown-6})][\text{OTF}]$ .

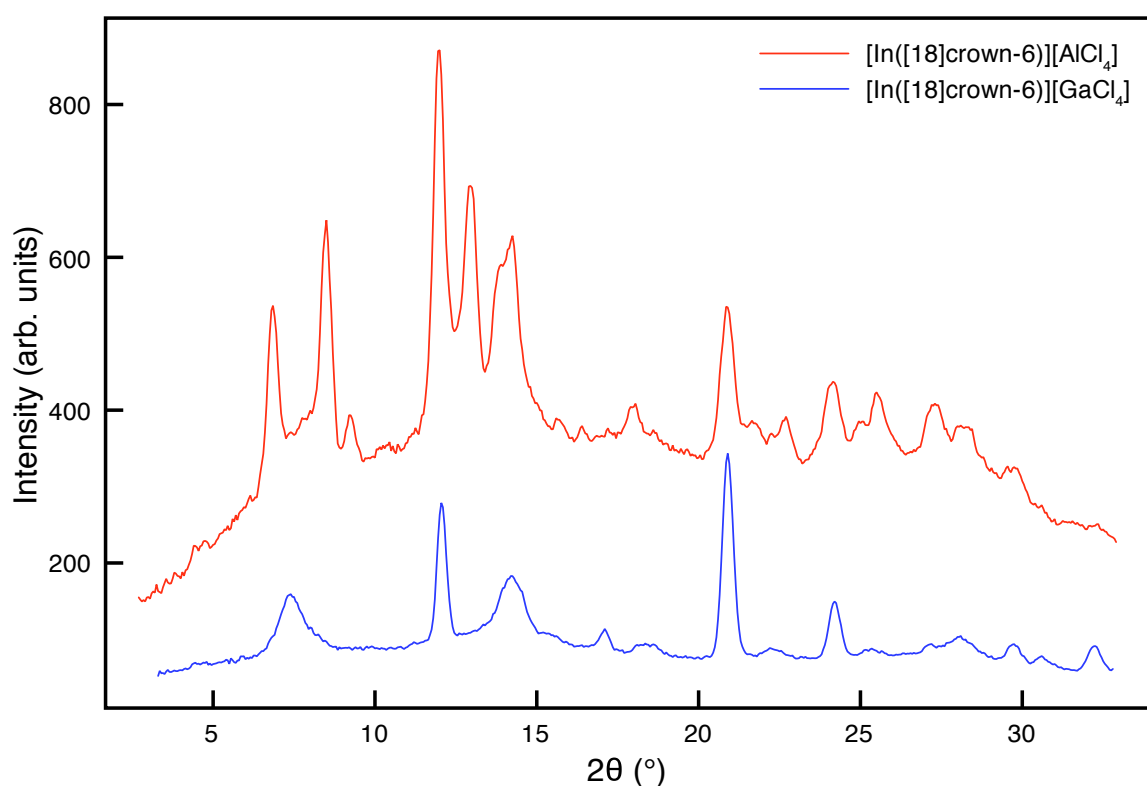


**Figure S8.** Powder X-ray diffraction patterns of  $[In([18]\text{crown-6})][\text{GaCl}_4]$  and  $[In([18]\text{crown-6})][\text{AlCl}_4]$  acquired at room temperature.

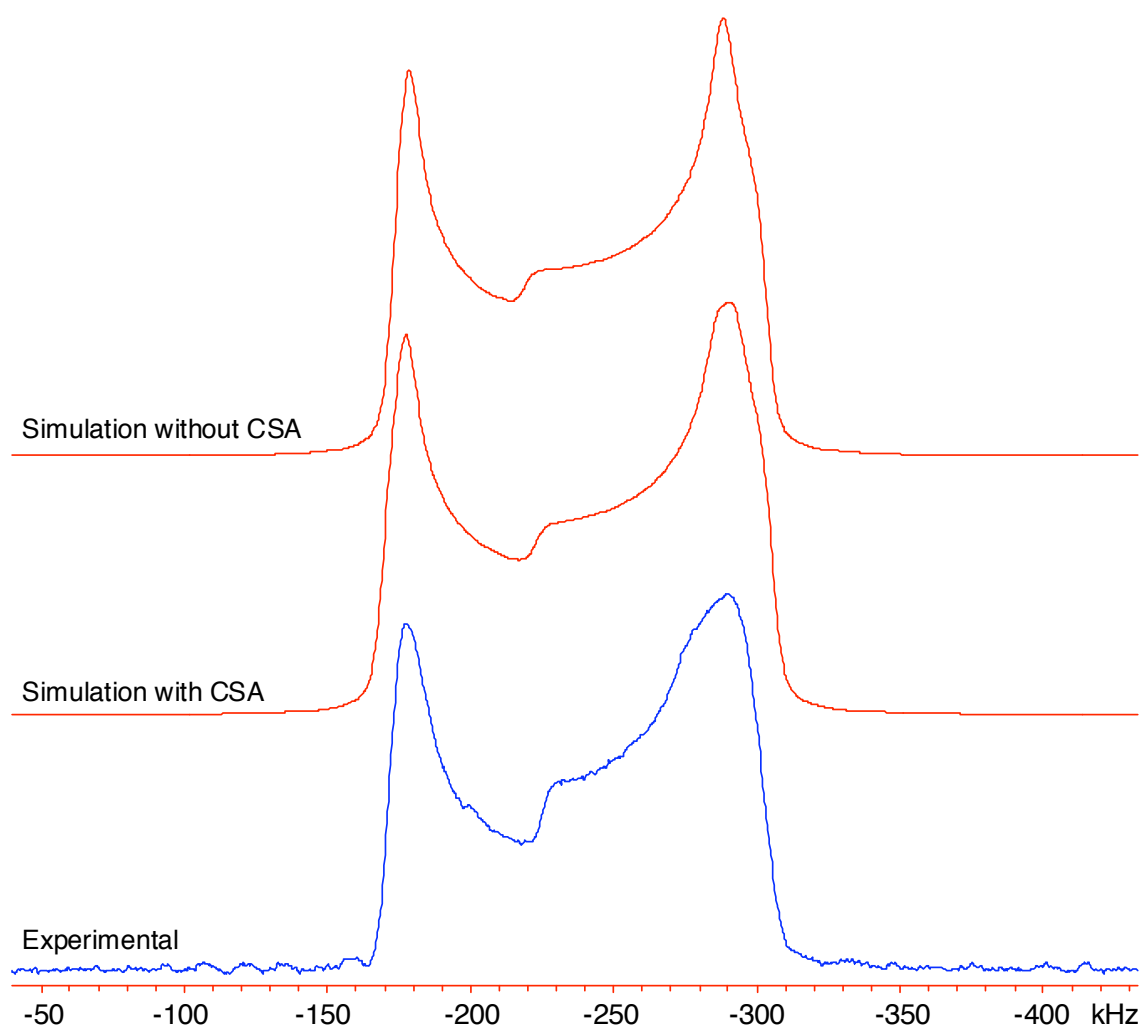


**Figure S9.** The contribution of  $^{115}\text{In}$  CSA on the NMR pattern of  $[\text{In}([\text{18}] \text{crown-6})][\text{GaCl}_4]$  acquired at 21.1 T.

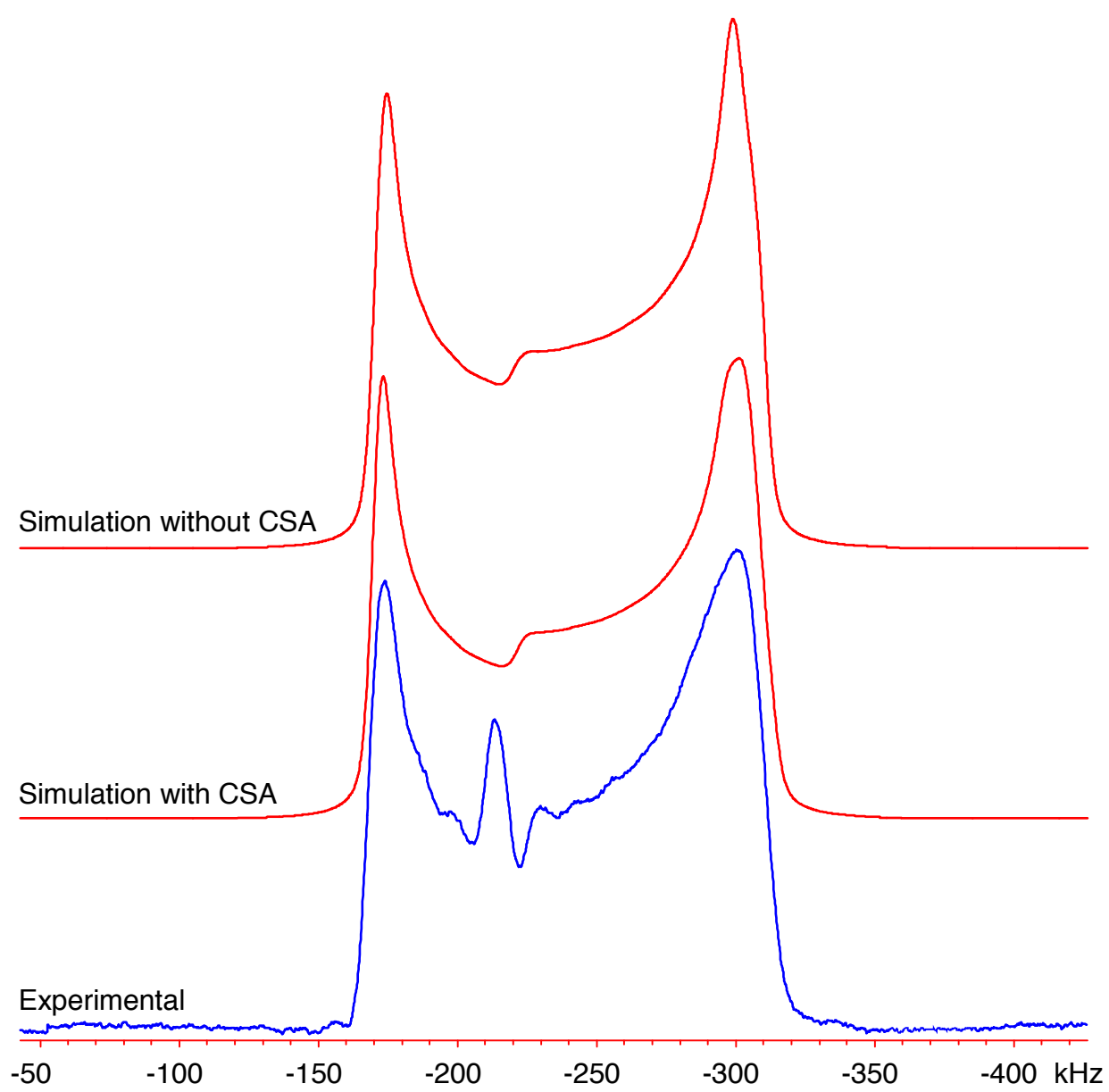


**Figure S10.** The contribution of  $^{115}\text{In}$  CSA on the NMR pattern of  $[\text{In}([18]\text{crown-6})]\text{AlCl}_4$ .

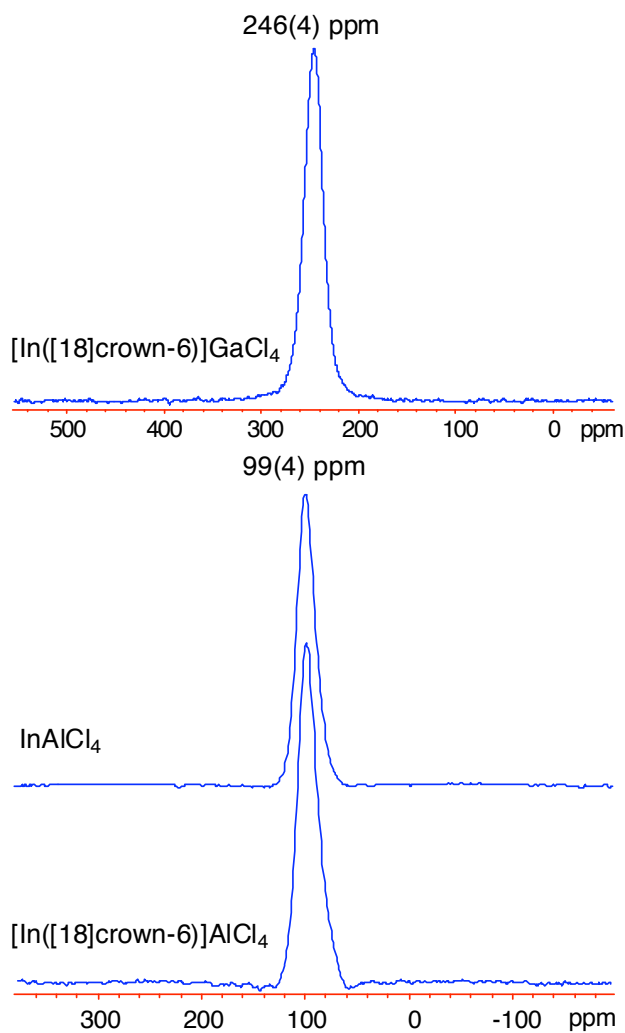


**Figure S11.** Static  $^{71}\text{Ga}$  SSNMR spectrum of  $[\text{In}([18]\text{crown-6})]\text{GaCl}_4$  and  $^{27}\text{Al}$  SSNMR spectra of  $\text{AlCl}_4$  and  $[\text{In}([18]\text{crown-6})]\text{AlCl}_4$  at 9.4 T.

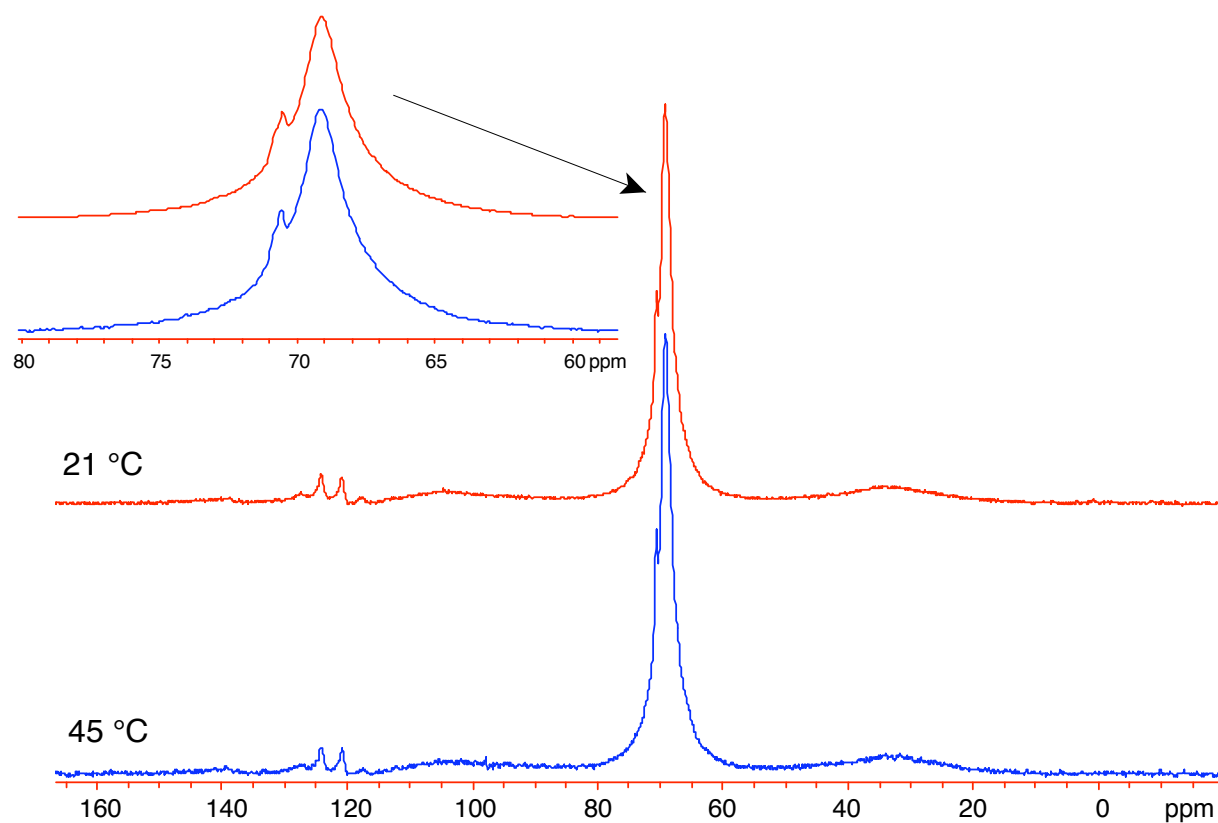


**Figure S12.** <sup>13</sup>C MAS NMR spectra of  $[\text{In}([\text{15}] \text{crown-5})_2]\text{[OTf]}$  at 21 °C and at 45 °C.

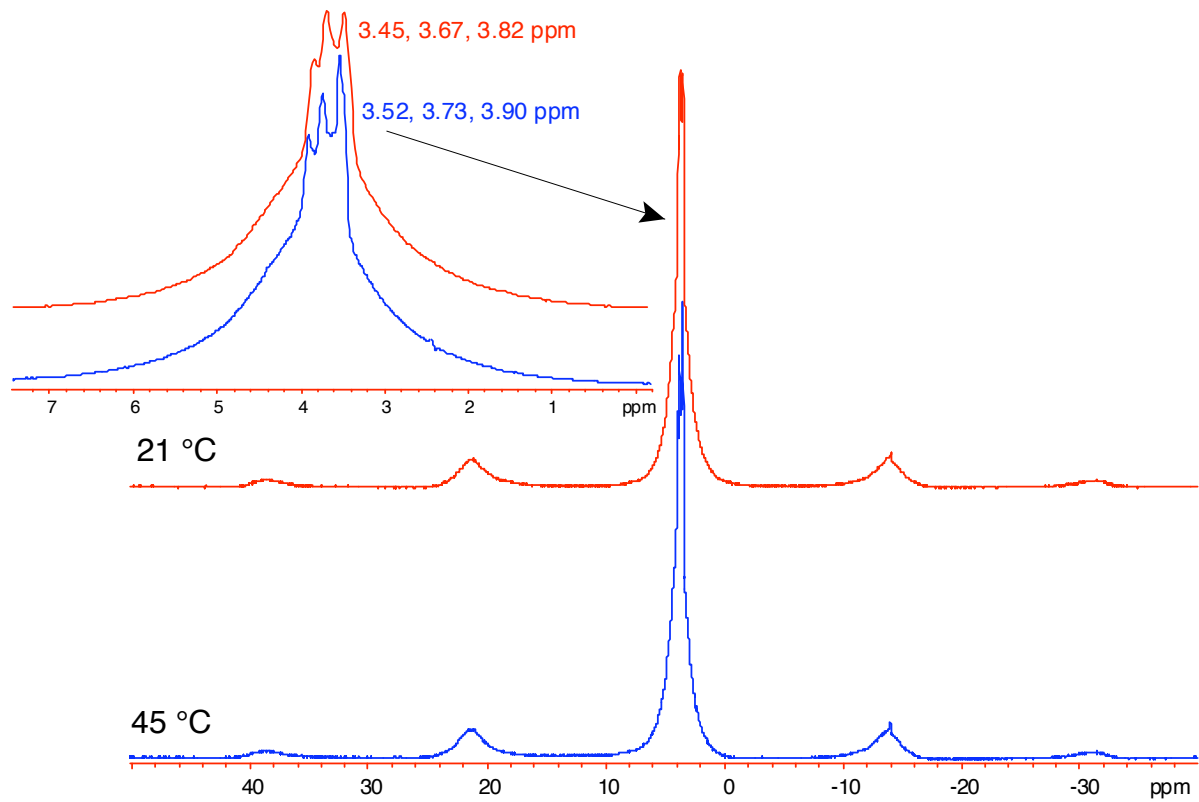


**Figure S13.** <sup>1</sup>H MAS NMR spectra of [In([15]crown-5)<sub>2</sub>][OTf] at 21 °C and at 45 °C.

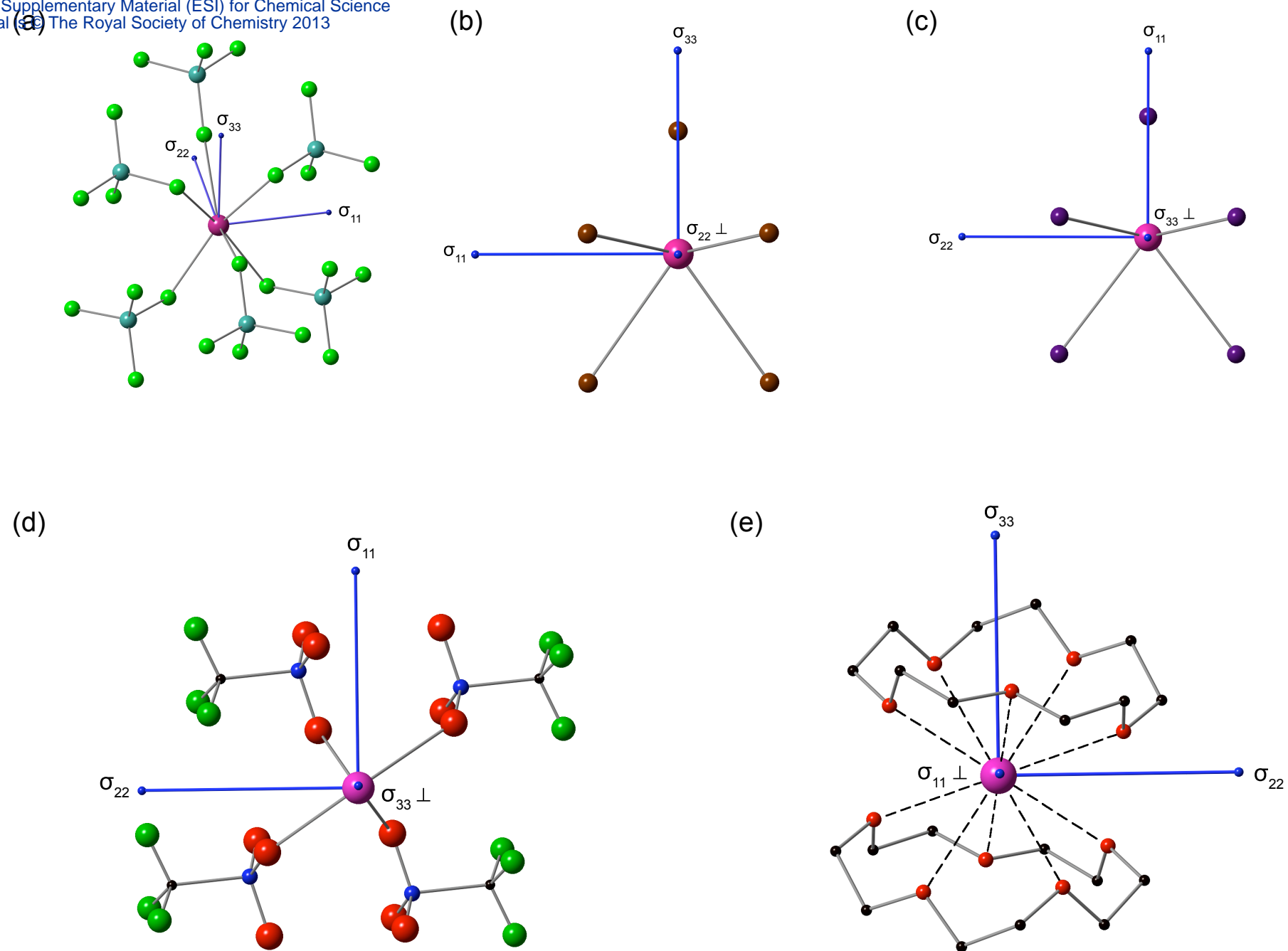


**Figure S14.** The  $^{115}\text{In}$  NS tensor orientations in (a)  $[In][\text{GaCl}_4]$ , (b)  $\text{InBr}$ , (c)  $\text{InI}$ , (d)  $[In][\text{OTf}]$  (In site 2) and (e)  $[In([15]\text{crown-5})_2][\text{OTf}]$ .